Development 126, 5421-5429 (1999)
Printed in Great Britain © The Company of Biologists Limited 1999
DEV8648

The *Drosophila* tissue polarity gene *starry night* encodes a member of the protocadherin family

Jeiwook Chae[1,3,*], Maeng-Jo Kim[1,*], Jae Hwan Goo[1], Simon Collier[2], David Gubb[2], Jeannette Charlton[3], Paul N. Adler[3] and Woo Jin Park[1,‡]

[1]Department of Life Science, Kwangju Institute of Science and Technology (K-JIST), Kwangju, 500-712, Korea
[2]Department of Genetics, University of Cambridge, Cambridge, CB2 3EH, UK
[3]Department of Biology and Cancer Center, University of Virginia, Charlottesville, VA 22903, USA
*The first two authors contributed equally to this study
‡Author for correspondence at address1 (e-mail: wjpark@eunhasu.kjist.ac.kr)

Accepted 7 September; published on WWW 9 November 1999

SUMMARY

The tissue polarity genes control the polarity of hairs, bristles and ommatidia in the adult epidermis of *Drosophila*. We report here the identification of a new tissue polarity gene named *starry night* (*stan*). Mutations in this essential gene alter the polarity of cuticular structures in all regions of the adult body. The detailed polarity phenotype of *stan* on the wing suggested that it is most likely a component of the *frizzled* (*fz*) pathway. Consistent with this hypothesis, *stan* appears to be downstream of and required for *fz* function. We molecularly cloned *stan* and found that it encodes a huge protocadherin containing nine cadherin motifs, four EGF-like motifs, two laminin G motifs, and seven transmembrane domains. This suggests that Stan functions in signal reception, perhaps together with Fz.

Key words: *Drosophila melanogaster*, Tissue polarity, *starry night*, *frizzled*, Protocadherin

INTRODUCTION

The adult cuticle of *Drosophila* is decorated with a large number of cuticular structures, such as hairs and bristles. These structures are polarized with respect to the plane of the epithelia and typically share a common polarity. For example, the wing is decorated with a large number of distally pointing hairs. Mutations in the tissue polarity genes disrupt the normal precise alignment of these structures (Gubb and Garcia-Bellido, 1982; Adler, 1992; Eaton, 1997). Most of the tissue polarity genes identified so far appear to be part of the *frizzled* (*fz*) signaling/signal transduction pathway, which controls the polarity of several types of cuticular structures (Adler, 1992; Gubb, 1993). Hair polarity is controlled by regulating the subcellular location for the initiation of the prehair – the cytoskeletal-mediated outgrowth that gives rise to the cuticular hair (Wong and Adler, 1993). In contrast, sensory bristle polarity is regulated by genes controlling the orientation of the cell divisions that give rise to the four cells of the bristle sensory organ (Reddy and Rodrigues, 1999; Gho et al., 1999). Ommatidia polarity is controlled by regulating the R3/R4 cell fate decision and the subsequent rotation of the developing ommatidia (Wherli and Tomlinson, 1998; Reifegerste and Moses, 1999). It is thought that there is a general tissue polarity intercellular signaling/signal transduction pathway that regulates specific downstream effector genes and proteins in the cells that give rise to the different cuticular structures (Adler, 1992).

The cadherins were originally identified as proteins that mediate Ca^{2+}-dependent cell adhesion. These proteins typically contain four or five extracellular cadherin motifs, a single transmembrane domain and a cytoplasmic tail that contains a binding site for β-catenin (reviewed in Geiger and Ayalon, 1992). Multiple tissue type-specific cadherin proteins are found in all animals. Epithelial cells typically contain E-cadherin, which is localized to the adherens junction and is essential for the maintenance of epithelial tissue structure. The ability of classical cadherins to mediate cell-cell adhesion requires their being linked to the actin cytoskeleton via the catenins (Nagafuchi and Takeichi, 1988). Since β-catenin (*armadillo* in *Drosophila*) is also a key member of the *wingless*/Wnt signal transduction pathway, cadherins can, at least indirectly, affect Wnt signaling (Peifer et al., 1991). The realization that *fz* encodes Wnt receptors provides a clue for potential connections between cadherins and catenins in the context of tissue polarity formation (Bhanot et al., 1996). However, it does not appear that *armadillo* or *shotgun* (the *Drosophila* E-cadherin gene) plays important roles in the development of wing tissue polarity (Peifer et al., 1991; Uemura et al., 1996; Tepass et al., 1996).

In addition to the classical cadherins, there is a diverse group of proteins called protocadherins that have been found in *Drosophila*, *C. elegans* and mammals. These proteins are often substantially larger than classical cadherins. For example, the *fat (ft)* protocadherin contains more than 30 cadherin domains (Mahoney et al., 1991). Relatively little is known about the

function of the protocadherins. Results of previous cell biological experiments suggest that protocadherins only weakly promote cell adhesion. The most interesting genetic data comes from the analysis of the *dachsous* (*ds*) and *ft* genes of *Drosophila*, which have recently been shown to encode protocadherins (Clark et al., 1995; Mahoney et al., 1991). Mutations in *ds* result in malformed flies that often die as pharate adults or as newly eclosed adults. The legs and wings are particularly abnormal in *ds* flies. Both are shorter and fatter than normal, and each also displays a number of specific defects including disrupted tissue polarity (Adler et al., 1998). Mutations in *ft* are pupal lethals. When clones of *ft* are generated in imaginal tissue, they result in tumorous outgrowths. Hence, *ft* appears to be a tumor suppressor gene in flies (Mahoney et al., 1991). Interestingly both *ds* and *ft* were among the genes identified in a large screen for new tissue polarity mutants. The underlying biochemical mechanisms by which mutations in these genes produce a tissue polarity phenotype are unknown. At the genetic level, it was shown that *ds* caused an altered anatomical direction of *fz* signaling and enhanced *fz* domineering nonautonomy (Adler et al., 1998).

The *starry night* (*stan*) gene was identified in the same mutant screen that led to the identification of *ds* and *ft* as tissue polarity genes. Mutations in *stan* produce a wing tissue polarity phenotype that is similar to that of *fz* and *dishevelled* (*dsh*; Krasnow et al., 1995), both in terms of the mutant wing polarity pattern and the small number of wing cells that produce more than the normal one hair. Genetic analyses in the present study have shown that *stan* likely plays a role in the *fz* signaling/signal transduction pathway that controls tissue polarity. Mutations that inactivate *stan* were found to spread across about 40 kb of genomic DNA. The *stan* gene produces a longer than 12 kb mRNA that encodes a protocadherin. This protein is homologous in general predicted structure to proteins identified in mammals (rMEGF2, mCelsr1) and *C. elegans* (CeCelsr). They contain a series of 8-9 cadherin motifs, 4-7 EGF-like motifs, two laminin G motifs, and a region of seven transmembrane domains that is reminiscent of trimeric G-coupled receptors (Hadjantonakis et al., 1997; Nakayama et al., 1998). The unusual structure of the Stan protein suggests it could function in both cell adhesion and cell signaling pathways.

MATERIALS AND METHODS

Fly culture and strains

Flies were grown on standard media at 25°C, unless stated otherwise. Many mutants were obtained from the stock center at the Indiana University. A chromosome carrying *Df(2R)17* was kindly provided by Dr R. Burgess (Stanford). Several different mutations that cytogenetically removed *stan* were used in our studies (*Df(2R)E3363, Df(2R)stan1, Df(2R)stan2, Df(2R)stan9, Df(2R)stan14, Df(2R)stan38*). For simplicity, they are all abbreviated as *Df-stan.* Alleles of *stan* were isolated independently in Charlottesville and Cambridge. In Charlottesville, the original *stan* alleles were identified in an F_1 FLP/FRT screen for new wing tissue polarity mutations, while the original allele identified in Cambridge was found in an unrelated mutant screen. Additional *stan* alleles were isolated in both locations by F_1 screens where we used a lack of complementation of viable alleles for screening. The alleles of *stan* were isolated by EMS, γ-ray, X-ray and P element mutagenesis. The gene was named *starry night* (*stan*) after the swirling brush strokes in the eponymous painting by Van Gogh.

Cytological procedures

To examine the process of hair morphogenesis, pupal wings were dissected in 4% paraformaldehyde/PBS, stained with a fluorescent-phalloidin which binds to F-actin (Wong and Adler, 1993) and examined by confocal microscopy (Molecular Dynamics).

Generation of genetic mosaics

Mosaic experiments were carried out using the FLP/FRT system to generate clones (Xu and Rubin, 1993). Larva of *w, hs-flp; FRT42 pwn stan/FRT42* were heat shocked at 38°C for 30 minutes to induce the recombination at the FRT site. The *stan* clones could be recognized by the recessive mutation *pawn* (*pwn*) that resulted in cells forming thin wispy hairs and short deformed bristles. Clones homozygous for *fz* were marked with the autonomously acting trichome morphology marker, *starburst (strb).*

Scoring of mutant wings

Wings from relevant flies were mounted in Euparal (Asco labs) and examined under bright-field microscopy. The analysis of wing phenotypes is described in detail elsewhere (Wong and Adler, 1993; Krasnow and Adler, 1994; Adler et al., 1994). A distal to proximal gradient of *fz* expression was induced by the 'waxing' procedure (Adler et al., 1997).

Molecular biology

P1 clones were generously obtained from Dr G. Rubin (UC Berkeley) and Dr E. Nitasaka (Kyushu University). P1 DNA was prepared by the alkaline lysis method described previously (Hartl et al., 1994) with slight modifications. DNA and RNA isolation, Southern analysis, northern analysis, genomic DNA and cDNA library screening was performed by standard methods (Sambrook et al., 1989). Genomic walking with λ clones was performed as described previously (Park et al., 1996). DNA sequencing was primarily done in the Core Center of the University of Virginia.

Seven RT-PCR were performed to obtain the full *stan* transcript. Reverse transcription was carried out using SuperScript Preamplification System (GIBCO-BRL). The resulting cDNA was subject to polymerase chain reaction that consisted of 35 cycles of denaturation for 30 seconds at 94°C, annealing for 1 minute at 55°C, and extension for 2 minutes at 72°C. For RT1 (1962 bp), the primer sets were 5′-ACT TGC GAG TGT GAT TCC-3′ and 5′-ATT TAG GCG AAT GTG TGG-3′; for RT2 (1918 bp), 5′-AGC TCC TTG GCG ATT CTC-3′ and 5′-CGG CAG CAC AAC ACT TTC-3′; for RT3 (1897 bp), 5′-ACG TAA CGA TGC CCA CAT-3′ and 5′-CTC TTT CTG GCG TGT TCG-3′; for RT4 (1598 bp), 5′-GTG TAC CAC CCA AAT CGG C-3′ and 5′-GGC TTC GTT AAT TCC ATC CG-3′; for RT5 (1861 bp), 5′-ACG CCT CCT ATG CCA TTC-3′ and 5′-AGC GAC TGG GCA ATG GTA-3′; for RT6 (1891 bp), 5′-GGC CTG CTC CTC GTG CT-3′ and 5′-TCA CAT CAC CGG ACA TCG-3′; for RT7 (1194 bp), 5′-TAG TCG TCG TGG CGT AG-3′ and 5′-CCT GTG TCT CAT CTC ATT GTC G-3′.

In situ hybridization

The 4,513 bp *stan* cDNA was digested with *Apa*I and *Sac*I, and the resulting 645 bp fragment was subcloned into pGEM-T-Easy vector (Promega). Sense and antisense RNA probes were prepared using the Dig RNA labelling kit according to the manufacturer's instruction (Boehringer Mannheim). In situ hybridization was performed as described previously (Tautz and Pfeiffle, 1989) with minor modification.

Sequence analysis

Genomic DNA sequence was analyzed for the presence of a putative open reading frame or exons using computer programs such as

WebGeneMarker and BCM gene finder (Smith et al., 1996). For RT-PCR, optimal primers were designed using Vector NTI (Informax) and Oligo 5.0 (National Biosciences). The PROSITE database was utilized for motif search of the Stan protein (Bairoch et al., 1997). The presence of putative signal peptide was determined using SignalP (Nielsen et al., 1997). Putative transmembrane domains were predicted using SOSUI (Hirokawa et al., 1998) and PHD (Rost et al., 1995) algorithms.

RESULTS

Isolation of *starry night* (*stan*) mutations

Mutations in the *stan* gene cause a tissue polarity phenotype over much of the epidermis. Epidermal hairs, sensory bristles and ommatidia are all affected by *stan* mutations, thus in this way *stan* resembles *fz*, *dsh*, *Van Gogh*(*Vang*)/*strabismus* (Taylor et al., 1998; Wolff and Rubin, 1998), and *prickle* (Gubb et al., 1999). We found the *stan* gene to be highly mutable. In one experiment, we simultaneously screened for mutations in *Vang*, *kojak* (*koj*) and *stan* after γ-ray mutagenesis. We isolated five times more *stan* (21 mutations) than *Vang* (4 mutations) mutations and seven times more *stan* than *koj* (3 mutations) mutations (P. N. Adler, unpublished). This suggested that *stan* was a large gene. The *stan* gene was mapped to position 62 on the second chromosome by meiotic mapping, and localized to 47B3-5 on the basis of several alleles that contained breakpoints in this interval and deficiencies that failed to complement *stan* point mutants (data not shown).

In our collection of 49 *stan* alleles, there is a great deal of phenotypic variation (a detailed description of the *stan* alleles and their genetic interactions with other tissue polarity genes will be presented elsewhere). Most *stan* mutations are recessive lethals. In this study, we made extensive use of $stan^3$, which is homozygous and hemizygous viable. Flies with this allele show a relatively strong polarity phenotype in the adult cuticle (Fig. 1B,D). The phenotype of $stan^3/stan^3$ wings is only slightly weaker than $stan^3$/*Df-stan* wings (compare Fig. 1G and H), thus by this criteria $stan^3$ is a strong hypomorphic allele for the wing tissue polarity phenotype. Since $stan^3$ is healthy, the mutation is presumably functional for the *stan* vital functions. It is possible that $stan^3$ is analogous to the dsh^1 mutation, which is defective for tissue polarity, but functional for the essential functions of this gene (Krasnow et al., 1995).

The *stan* wing phenotype

We have used viable *stan* mutants (particularly $stan^3/stan^3$ and $stan^3$/*Df-stan*) to examine the *stan* wing phenotype. As is the case for other tissue polarity mutants, *stan* mutants do not show a complete loss or randomization of hair polarity across the wing. Rather, they show a stereotypic abnormal polarity pattern (Fig. 1B,G,H). As noted previously, the polarity patterns that result from mutations in many tissue polarity genes are quite similar, albeit not identical. We call this pattern the *fz*/*inturned (in)* pattern after two of the best-studied genes in *fz* pathway (Fig. 1F). The *stan* mutant wings also have this general pattern. A second criterion that we have used to characterize tissue polarity mutants is the frequency of wing cells that form more than the normal one hair. Wings homozygous for $stan^3$ have relatively few multiple hair cells (an average of 1.03 hairs/cell in our typical test region). This is similar to wings mutant for

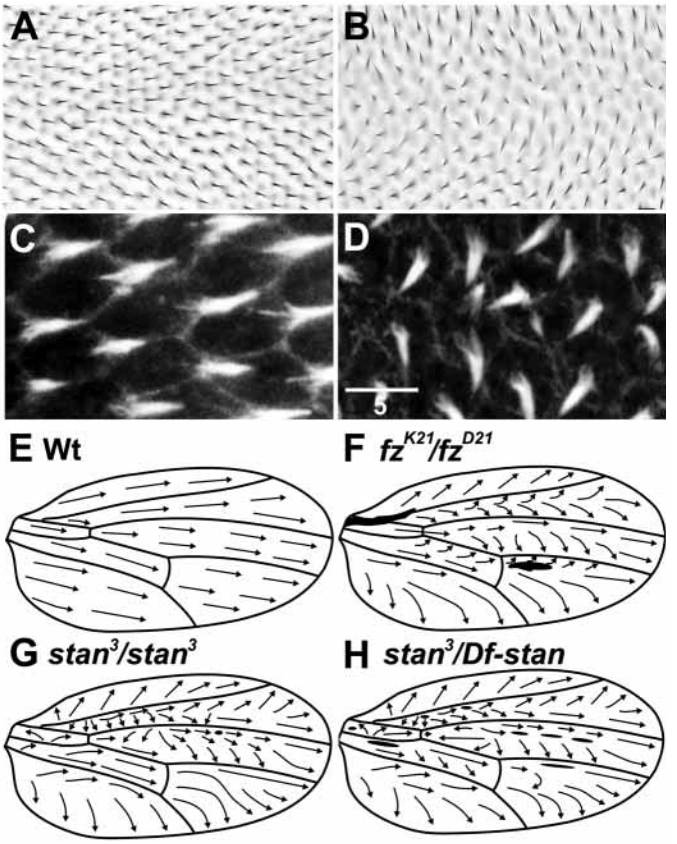

Fig. 1. Wing phenotype of *stan.* A and B are light micrographs of wings from wild-type and $stan^3/stan^3$ flies, respectively. C and D are confocal images of wild-type and *stan* pupal wings, respectively. Note that prehairs are initiating at central locations on the apical surface of the *stan* wing cells, whereas the prehairs form in the vicinity of the distal most vertex of the wild-type wing cells. Several cells in this field have formed two hairs. E, F, G and H are drawings of the polarity pattern on the dorsal surfaces of wild-type, fz^{K21}/fz^{D21} (this represents the *fz* null phenotype on the wing), $stan^3/stan^3$, $stan^3$/*Df* wings, respectively. Note the phenotype in H is only slightly stronger than that in G.

fz (1.02 hairs/cell), *dsh* (1.01 hairs/cell) and *pk* (1.02 hairs/cell). In contrast, it is much lower than that seen in wings mutant for *inturned (in)* (1.82 hairs/cell), *fuzzy (fy)* (1.92 hairs/cell) and *multiple wing hair (mwh)* (3.94 hairs/cell). We have also examined the process of hair morphogenesis in *stan* pupal wings. In wild-type wings, the prehairs that develop into the adult cuticular hairs are formed in the vicinity of the distal-most vertex of the cell and extend away from the cell in a distal direction (Fig. 1C). In *stan* mutants, many cells formed prehairs at a relatively central location on the apical cell surface (Fig. 1D). Other cells formed prehairs at abnormal locations along the cell periphery. This is similar to what we have found for mutations in the *fz*-like genes (Wong and Adler, 1993). Thus, based on several phenotypic criteria we place *stan* in the *fz*-like group of genes.

Cell autonomy of wing clones

Several recessive *stan* alleles were isolated due to a wing hair polarity phenotype seen in a wing in an FLP/FRT based F_1 screen. Thus, it was clear that the presence of wild-type

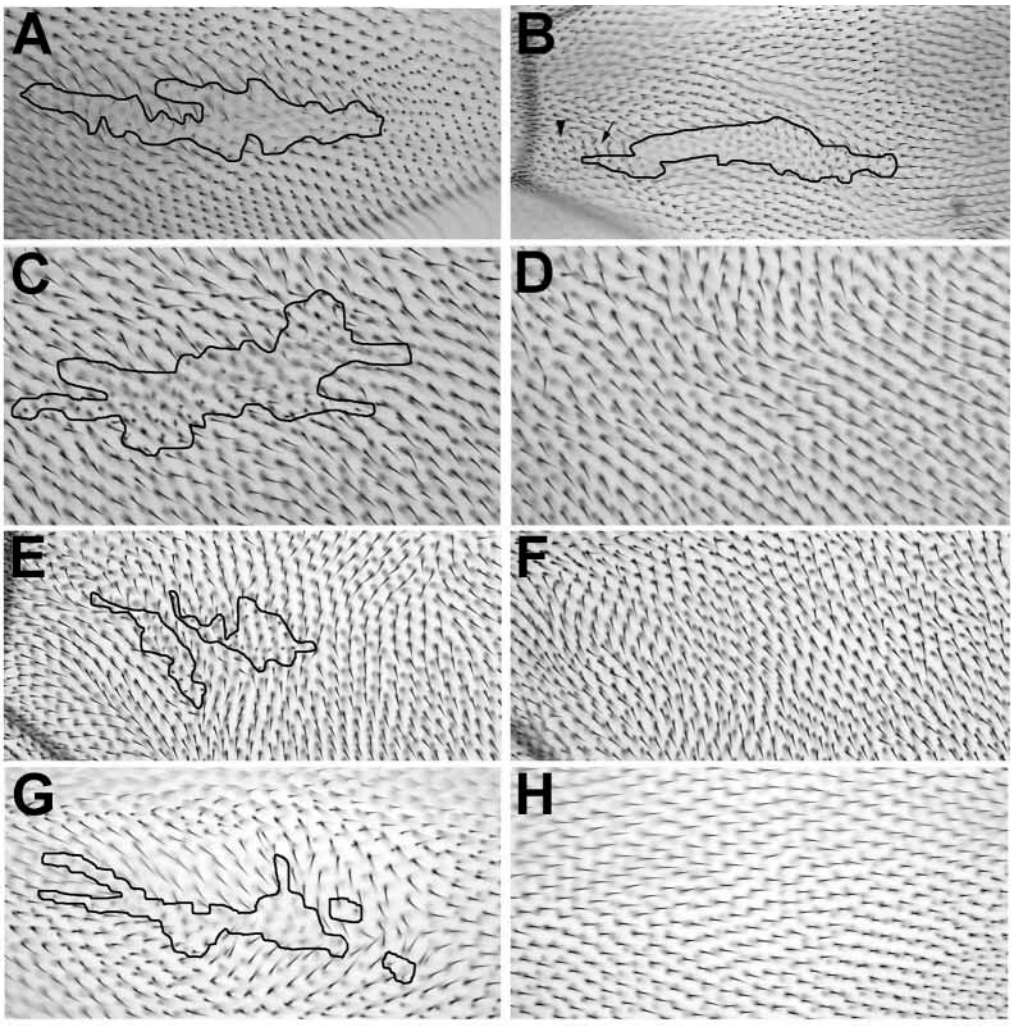

Fig. 2. Mitotic clone analysis. A and B show *pwn stan*^{24} somatic clones. The clone in A behaves cell autonomously as do most *stan* clones. The clone in B shows the weak domineering non-autonomy displayed by a minority of *stan* clones. The arrow points to several hairs with abnormal polarity that are not juxtaposed to the clone. The arrowhead indicates a cell that has formed two hairs. C and E show *fz*^{R52} *strb* clones in *stan*^{3} wings. Equivalent regions of sibling wings where there are no clones are shown in D and F for comparison. The typical domineering non-autonomy of the *fz* clones in wild-type wing is shown in Fig. 1G. H shows the equivalent region of a wild-type wing.

neighboring cells would not rescue all of the mutant cells in a clone. Several of the tissue polarity genes display domineering nonautonomy in wing clones – that is the presence of mutant cells in a clone alters the development of wild-type cells that are near the clone. To see if *stan* clones also displayed domineering nonautonomy, we generated mosaic wings where *stan* clones were marked with the hair marker *pwn*. Several different alleles were tested including the putative null allele *stan*^{24}, the recessive lethal allele *stan*^{21} and the recessive viable allele *stan*^{3}, and similar results were obtained. In all cases, the majority of clones behaved cell autonomously (53/60 for *pwn stan*^{21} clones, 72/83 *pwn stan*^{24} clones and 19/22 *pwn stan*^{3} clones) (Fig. 2A). Further, the extent of domineering nonautonomy for those clones scored as showing it was typically much weaker than we have seen with *fz* or *Vang* (Fig. 2B). We conclude from these experiments that *stan* principally functions cell autonomously.

stan suppresses the domineering non-autonomy of *fz* clones

As an in vivo assay for *fz* pathway function, we used the domineering non-autonomy of *fz* clones. To do this, we induced *fz*^{R52} *strb* clones in *stan*^{3} wings. In a wild-type wing, more than 80% of *fz* clones show distal domineering non-autonomy. That is, cells distal (and in part anterior/posterior) but not proximal to the clone show altered polarity that extends to cells that do not border the clone (Fig. 2G,H). We scored 54 *fz*^{R52} *strb* clones in regions of *stan*^{3} wings, where the polarity was consistent enough for us to be able to score the clones for domineering non-autonomy. Forty two clones behaved cell autonomously (Fig. 2C,D) and only 12 clones showed evidence of domineering non-autonomy. Further, the extent of domineering non-autonomy in these 12 clones was modest (Fig. 2E,F). Thus, *stan* appears to be a suppressor of the domineering non-autonomy of *fz*. That there remains some *fz* domineering non-autonomy in *stan*^{3} wings may reflect *stan*^{3} not being a null allele. The ability of a *stan* mutation to suppress this *fz* phenotype argues that *stan* is downstream of *fz* and required for the cell non-autonomous function of the *fz* pathway.

stan is required for the ability of a gradient of *fz* expression to repolarize wing hairs

As a second in vivo assay for *fz* pathway function, we used the ability of a gradient of *fz* expression, with its highest point near the distal tip of the wing, to reverse the normal distal polarity of wing hairs (Adler et al., 1997). This result argues that cells can ‘sense’ the *fz* activity of neighboring cells and respond to this information. The production of a region of reversed polarity is likely to require both cell non-autonomous (e.g., a *fz*-dependent intercellular signal) and cell autonomous

functions (e.g., transduction of the *fz*-dependent signal). We found that *stan*^{3} completely blocked the ability of a gradient of *fz* expression to reorganize wing hair polarity (Table 1). Hence we conclude that *stan* functions downstream of *fz* and is required either for the cells to be able to sense the *fz* activity of neighboring cells or to respond to this information.

Table 1. *starry night* function is required for a gradient of *frizzled* expression to produce a region of reversed wing hair polarity

Genotype	Number of wings with regions of reversed polarity	Number of wings showing other effects on polarity	Number of wings showing no effect of waxing on polarity
stan^{3}	0	0	29
stan^{3}; *hs-fz*	0	2	19
hs-fz	41	6	4

stan does not block the late *fz* gain of function

The overexpression of *fz* just prior to prehair initiation causes the formation of large numbers of multiple hair cells that are a phenocopy of the *in*-like mutations (Krasnow and Adler, 1994). We have previously used this *fz* gain-of-function phenotype as a test to identify genes that are downstream of and required for the transduction of the *fz* signal (Krasnow et al., 1995). It was shown that the function of the *dsh* gene, which is thought to function downstream of *fz* (Klingensmith et al., 1994; Theisen et al., 1994), was indeed required for this phenocopy (Krasnow et al., 1995). However, the function of several other tissue polarity genes, *pk*, *ds* and *Vang*, was not required (Krasnow et al., 1995; Adler et al., 1998; Taylor et al., 1998). To determine if *stan* was required for the transduction of the *fz* signal, we constructed *stan*; *hs-fz* flies and induced *fz* expression just prior to prehair initiation. We found that the *stan*^{3} did not block the ability of *fz* overexpression to induce cells to form multiple hairs (Table 2). Rather, it appeared to slightly enhance the ability of *fz* overexpression to induce multiple hair cells.

Mapping of the *stan* locus

We initially mapped *stan* to 47B2-4 based on the cytogenetic analysis of two independent *stan* inversions, *stan*^{10} and *stan*^{35} (data not shown). P1 clones covering this region were obtained and used to screen a *Drosophila* genomic λ phage library. The clones were assembled into a contig covering about 76 kb and a restriction map was constructed (Fig. 3). RFLPs associated with *stan*^{10} and *stan*^{35} were identified by genomic Southern blot analysis, and these were found to be separated by approximately 40 kb, consistent with the large genetic target size of *stan*. We also identified RFLPs associated with two cytologically normal alleles (*stan*^{15} and *stan*^{24}) induced by treatment with ionizing radiation. Both mapped in the GC5 region relatively close to the RFLP associated with *stan*^{35}.

Identification of the *stan* transcript

To identify and map gene products in the putative *stan* locus, northern blots were screened with the inserts of all the λ phage clones. Distinct RNA bands of 4.9 kb, >10 kb, and 3.8 kb in length were detected with the inserts from the clones GC71, GC5 and GC1 respectively. A late embryonic cDNA library

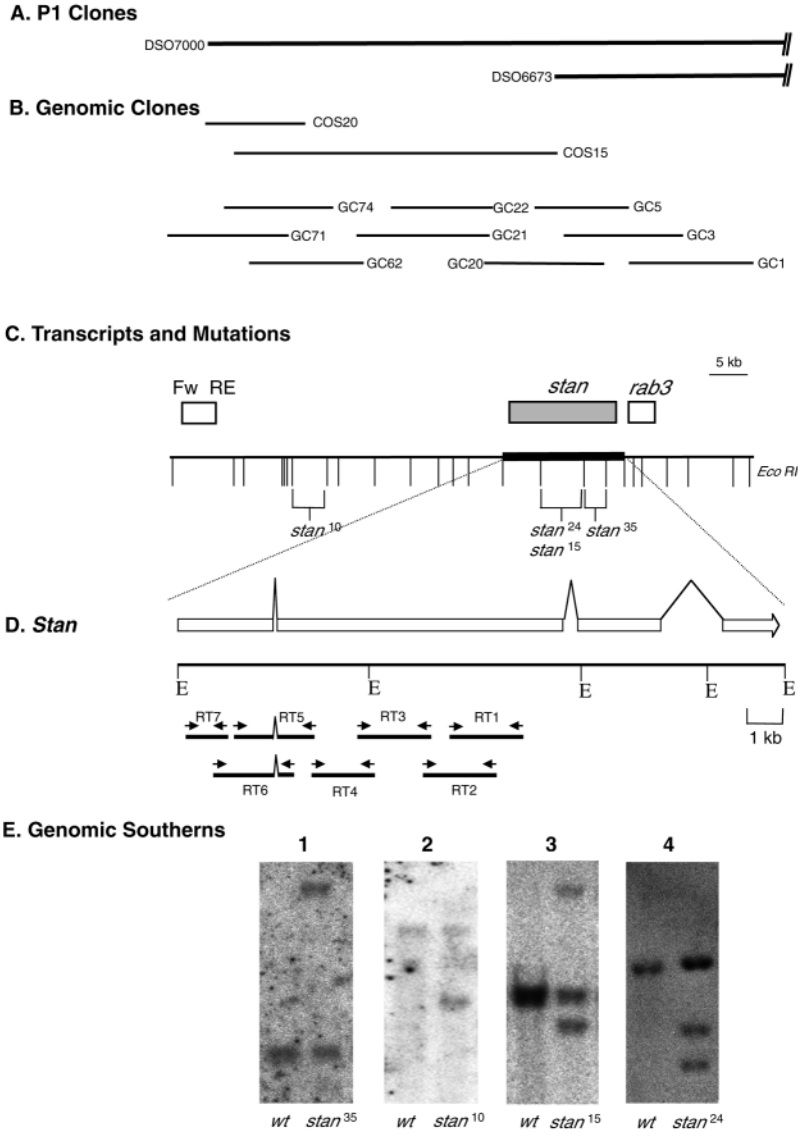

Fig. 3. Molecular cloning of *stan*. A represents two P1 clones used for initial molecular characterization of the *stan* locus. B shows a contig of cosmid and λ phage clones. C shows a restriction map of the *stan* locus made with *Eco*RI, the locations of *stan* and two unrelated transcripts, and the locations of the four *stan* mutations as determined from genomic Southern analysis. D shows the structure of the *stan* cDNA. Also shown are the regions of the *stan* cDNA that were confirmed by RT-PCR. E shows representatives of the genomic Southern analysis of *stan* mutations. 1 is an *Eco*RI digestion of wild-type and *stan*^{35} genomic DNA probed with a 3.5 kb *Eco*RI fragment of GC5. 2 is a *Nde*I digestion of wild-type and *stan*^{10} genomic DNA probed with a 4.4 kb *Eco*RI fragment of GC62. 3 is an *Eco*RI digestion of wild-type and *stan*^{15} genomic DNA probed with a 5.2 kb *Eco*RI fragment of GC5. 4 is an *Eco*RI digestion of wild-type and *stan*^{24} genomic DNA probed with a 5.2 kb *Eco*RI fragment of GC5.

(Brown and Kafatos, 1988) was then screened with probes from these clones. We isolated cDNA clones representing these three independent mRNAs and sequenced members of each cDNA class. One group (obtained after screening with GC71) was found to have 93% sequence identity to the Fw repetitive elements found in the *white* locus of w^i flies. These sequences show an extensive sequence similarity to L1 sequences, a major family of repetitive DNA elements dispersed in the mammalian genome (Di Nocera and Casari, 1987). The second group was found to encode the *Drosophila rab3* gene, which was previously mapped to 47B1-14 (Johnston et al., 1991).

The third group was represented by a 4.5 kb cDNA that hybridized to a larger than 10 kb mRNA on northern blots, suggesting it was an incomplete cDNA. Sequencing showed that it encoded part of a novel protein. A consensus poly(A) signal (AATAAA) was found and followed by a stretch of poly(A) tail, implying that the cDNA contains a true 3′ end. The cDNA mapped to restriction fragments altered by three of the *stan* RFLPs arguing that it was a product of the *stan* gene. To identify the remainder of the *stan* transcript, we sequenced genomic DNA encompassing about 50 kb and identified potential coding regions by computer analysis. We then used RT-PCR to test if the identified regions were indeed found in *stan* mRNA and they were present in the same RNA molecule as our original cDNA clone. The RT-PCR products were sequenced to confirm the predicted structure of *stan*. As summarized in the Fig. 3, the *stan* gene consists of at least four exons, and the *stan* mRNA is over 12 kb in length encoding a putative 3,579 amino acid protein.

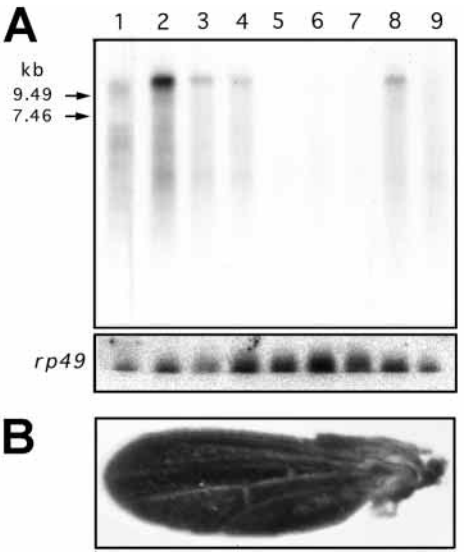

Fig. 4. Expression of *stan*. A shows a developmental northern blot. About 5 μg of poly(A) RNA from various developmental stages was fractionated and blotted to Nytran. The blot was probed with the original 4.5 kb *stan* cDNA. The lower panel is the same blot reprobed with *rp49* as a loading control. Lane 1, 0-3 hour embryo; lane 2, 6-9 hour embryo; lane 3, 9-12 hour embryo; lane 4, 12-24 hour embryo; lane 5, first instar larva; lane 6, second instar larva; lane 7, third instar larva; lane 8, 1 day pupa; lane 9, adult. B shows an in situ hybridization of pupal wings with *stan*. The pupal wing was prepared and hybridized with an antisense *stan* RNA probe as described previously (Tautz and Pfeiffle, 1989).

stan expression

Northern blot analysis showed that the large *stan* mRNA was present in a number of developmental stages (Fig. 4A). It was most abundant in 6-9 hour embryos and more abundant in pupae than larvae. We used in situ hybridization to examine the expression of *stan* in pupal wings. We found *stan* mRNA to be present at relatively even levels in all regions of the pupal wing (Fig. 4B). This is consistent with the genetic experiments showing that *stan* mutations have a phenotype over most if not all of the wing.

The Stan protein is a protocadherin

The conceptual translation of the *stan* mRNA yielded a protein with several notable motifs (Figs 5, 6). When analyzed with SignalP algorithm (Nielsen et al., 1997), the amino-terminal peptide consisting of the first 29 amino acids was predicted to serve as a signal peptide. This and the presence of seven putative transmembrane domains in the carboxy terminus suggest that Stan is a type 1 membrane protein. In addition, the huge extracellular part of the protein contains nine cadherin motifs, two laminin G motifs, and four EGF motifs implying that Stan may communicate with many signaling molecules or receptors. Database searches showed that *stan* is closely related to mammalian genes, rMEGF2 (Nakayama et al., 1998) and mCelsr1 (Hadjantonakis et al., 1997) and a *C. elegans* gene, CeCelsr. Their function is largely unknown except that rMEGF2 is specifically expressed in cerebellum and olfactory bulb (Nakayama et al., 1998) and mCelsr1 is expressed in the developing central nervous system (Hadjantonakis et al., 1998). While carrying out the molecular analysis of *stan*, we learned that the same gene had been cloned by the Uemura group (Kyoto University) due to the cadherin domain homology (Usui et al., 1999). They have called the gene *flamingo* and obtained cell biological data showing that *flamingo* is downstream of *fz*.

Table 2. *stan* does not block the ability of *fz* overexpression to induce multiple hair cells

	Genotype					
	Stan^3	*stan*^{3}	*stan*^{3}; *hs-fz*	*stan*^{3}; *hs-fz*	*hs-fz*	*hs-fz*
Heat shock	No	Yes	No	Yes	No	Yes
Mean number of mhcs* (s.d.)	13.6 (9.6)	20.6 (14.1)	18.7 (13.5)	181.8 (122.7)	0 (0)	46.6 (42.2)
Number of wings	5	10	8	9	5	10
Effect of heat shock	NR$^{\#}$	No (P=0.43)	NR$^{\#}$	Yes (P=0.002)	NR$^{\#}$	Yes (P=0.017)

*Number of multiple hair cells in the dorsal A region of the wing (Krasnow et al., 1995).
$^{\#}$Not relevant.

DISCUSSION

stan interacts with *fz*

Several lines of evidence point to *stan* function being required for the function of the *fz* pathway in wing tissue polarity. Mutations in *stan* produce an abnormal polarity pattern that is typical of tissue polarity genes whose function is thought to be essential for the pathway, such as *fz* and *dsh*. We also found a number of strong genetic interactions between *stan* and several *fz* pathway genes, including an allele-specific interaction between *stan* and *fz* (data not shown). Further, the domineering non-autonomy of *fz* is strongly suppressed by the $stan^3$ mutation (Fig. 2). Finally, the ability of a directed gradient of *fz* expression to redirect the polarity of cells on the wing is blocked by the $stan^3$ mutation (Table 1). All of these observations argue that *stan* function is essential for the function of the *fz* pathway.

Since *stan* mutations do not block the ability of the late overexpression of *fz* to produce an *in*-like phenotype (Table 2), the interaction between *fz* and *stan* is complex. It appears that *fz* carries out multiple (both cell autonomous and non-autonomous functions) roles in tissue polarity. The requirement for *stan* function for some but not all *fz* functions provides further evidence that *fz* has multiple roles in the development of tissue polarity. The two functions of *fz* could represent *fz* functioning in two distinct pathways or *fz* functioning at two times/locations in a single pathway. In the former model *stan* could be downstream of *fz* in one of the two pathways, and in the latter model it could function between the two times/locations where *fz* functions and hence be downstream of some *fz* functions and upstream of others. The requirement for *stan* function for a gradient of *fz* expression to redirect wing hair polarity and for the domineering nonautonomy of *fz* clones, but not for the late overexpression of *fz* to induce an *in*-like phenotype is not unique to *stan*, but is also a property of *Vang* (Taylor et al., 1998).

The Stan protein has multiple domains

Conceptual translation of the *stan* open reading frame reveals that it encodes a member of a protocadherin family found in both mammals and *C. elegans*. The protein has a remarkable structure that includes nine cadherin motifs, four EGF motifs, two laminin G motifs and seven transmembrane domains. The protocadherins are not nearly as well studied as classical cadherins, and relatively little is known about their in vivo function. The classical cadherins were identified as proteins that mediated Ca^{2+}-dependent cell adhesion (reviewed by Geiger and Ayalon, 1992). E-Cadherin is present at adherens junctions in epithelial cells and is essential for the maintenance of tissue structure. Cadherin-dependent cell adhesion requires the linkage of the cadherin to the actin cytoskeleton, which is mediated by the catenins (Nagafuchi and Takeichi, 1988). Some protocadherins, such as Ds and Ft have potential catenin binding sites although these are interrupted (Clark et al., 1995; Mahoney et al., 1991). Stan does not apparently have such catenin binding sites. Ds and Ft have been suggested to have an adhesion function based on a number of phenotypes. For example, large *ft* clones in the wing often end up evaginating inward to form cuticular nodules. This might be a consequence of altered adhesion. Smaller *ft* clones as well as *ds* clones exhibit a marked tendency to assume an oval shape, once again consistent with the hypothesis that the clone cells have altered adhesivity (P. N. Adler, unpublished data). In contrast, we saw no such phenotypes with *stan*. Hence, we think it unlikely that *stan* mutations have a major effect on the adhesion of wing cells. However, we note that the Uemura group has obtained evidence for *stan* being an adhesion protein in cultured cells (Usui et al., 1999).

```
MQTRFFPQRFLGLLVLLVLLQSLIKSYLIIVHEDTPPGTVIFNASVYKLGSERHYKI 60
NAHKSANFVHHLVSVNHKDGQIQLRKALKCDGIYYPNLFTFYVDSTSNRLRSIDYYSLPV 120
RIFVSGHSCNEDRRIEQELHHHHYEEEDNTGYSKRRRRRSTQEMIQLNGNQLEEVFRQNS 180
SEFRAGDLIFGDSFDNEMRHRILSRKRRAVGSPDPLHLQPALHRRISDAKQWISETYASY 240
AIHTTDKWNQICLRRSQFINSLNAFLPRSVCQHCKVSFLDVNDERFAIEHQSRDLVASRD 300
VCIAESMWKVSITFNIRCDRRDIVDSDHRLKIVYHHQEFNDTDIARRVRRELRNQSPYFE 360
LALYVASVLEEQPAGAAVTTVRARDPEDSPVVYSMVSLLDSRSQSLFKVDSRTGVVTTSA 420
SLDRELMDVHYFRVVATDDSFPPRSGTTTLQVNVLDCNDHSPTFEAEQFEASIREGATVG 480
STVITLRATDQDIGKNAEIEYGIEAVTDGAGLAQDQEMPIFRIDSRSGVISTRSSLDRET 540
SDSYHLLVTAADLASAQSERRTATASVQVKVLDDNDNYPQFSERTYTVQVPEDQWGGTED 600
NTVAHIRATDADQGNNAAIRYAIIGGNTQSQFSIDSMSGDVSLVKPLDYESVRSYRLVIR 660
AQDGGSPSRSNTTQLLVNVIDANDNAPRFYTSQFQESVLENVPVGYNIIRVQAYDSDEGA 720
NAEITYSISERDDDNFPLAVDPRTGWVQTIKPLDREEQGRFAFQVVAKDGGVPPKSASSSV 780
VITVQDVNDNDPAFNPKYYEANVGEDQPPGTPVTTVTATDPDEDSRLHYEITTGNTRGRF 840
AITSQNGRGLITIAQSLDYKQEKRFLLTVAATDSGGRSDTATVHINITDANNFAPIFENA 900
PYSASVFEDAPVGTTVLVVSATDSDVGVNAQITYSLNEESINGLGSPDPFSINPQTGAIV 960
TNAPLDRETTSGYLLTVTAKDGGNPSLSDTTDVEIGVTDVNDNAPAFKSPLYQASILEDA 1020
LVGTSVIQVAASDPDVGLNGRIKYLLSDRDIEDGSFVIDPTSGTIRTNKGLDRESVAVFH 1080
LTAIAVDKGSPPLSSTVEVQIRLEDVNDSPPTFASDKITLYVPENSPVGSVVGEIHAHDP 1140
DEGVNAVVHYSIIGGDDSNAFSLVTRPGSERAQLLTMTELDYESTRKRFELVVRAASPPL 1200
RNDAHIEILVTDVNDNAPVLRDFQVIFNNFRDHFPSGEIGRIPAFDADVSDKLHYRILSG 1260
NNANLLRLNSSSGGLVLSPQLNTNVPKFATMEVSVSDGINEAKAIMQLSVRLITEDMLFN 1320
SVTVRLNEMTEEAFLSPLLNFFLDGLAAIIPCPKEHIFVFSIQDDTDVSSRILNVSFSAR 1380
RPDVSHEEFYTPQYLQERVYLNRAILARLATVEVLPFDDNLCVREPCLNFEECLTVLKFG 1440
NASEFIHSDTVLFRPIYPVNTFACSCPEGFTGSKEHYLCDTEVDLCYSDPCQNGGTCVRR 1500
EGGYTCVCPSTHTGQNCETGVGHLRPCPSETCEGGLSCLSNYPSSQPPPYTATCELRARA 1560
FGRNSFLTFESLKQRHRFNLKLRFATVQENGLLLYNGRYNELHDFIALEIHEGHVSFSFS 1620
LGDHSERISVIQEAKVSDGKWHQVEVVYLNRSVTLVLDNCDTAIALSGQLGDRWSCANRT 1680
TLKLDKRCSLLTETCHRFLDLTGPLQVGGLPRIPAHFPVTNRDFVGCISDLRIDDRFVDL 1740
NSYVADNGTLAGCPQKAPLCQSEPCFNGGTCREGWGTYSCECPEGYAGNSCQDNIPAPWR 1800
FSGDGSLSFNPLLRPIQLPWTTSFSLRTRQKEAFLLQIQIGQNSSAAVCLRQGVLYYIFD 1860
GEPMYLAGAFLSDGEWHRVEIRWQQGSEIHFSVDYGQRSGSVPMSQKVQGLYVGKIVMGS 1920
PDGSIGAVPEASPFEGCIQDVRIGAGQSVLSRPTIRENVEDGCESRAHCPDHCPNHSSCQ 1980
SSWDLSTCECDSGYVGTDCAPICTVRPCASGVCRANTSLPRGYDCECNSSSRHGDYCEKE 2040
LQQPCPGGWWGERVCGPCRCDLAQGYHPDCNKTTGQCYCKTNHYQPPNETACLSCDCYSI 2100
GSFSGACNPLTGQCECREGVIGRRCDSCSNPYAEVTLSGCEVVYDACPRSFAGGVWWPRT 2160
PLGGVAIEGCPPPARGKGQRSCDVQSGSWNTPDMYNCTSEPFVELRRQLSQLEKLELELN 2220
SFVAIKMAEQLRKACEAVDRRGASKDQKISGNGRPNRRYKMESSFLLSNGENVWSHELEM 2280
DYLSDELKFTHDRLYGADLLVTEGLLQELINYELMQSGLNLSHSQDKYFIKNLVDAASVI 2340
LDRKYEAEWRRATELIQRGPDDLVDAFNKYLVVLARSQHDTYTSPFEIVQPNMALGLDIV 2400
TTESLFGYEPEQLSEYHRSKYLKPNAFTTESVVLPDTSGFLQHSARQRPVISFPKYNNYI 2460
LDRRKFDQHTKVLVPLEMLGITPPESDEISQSGRRGSSHDHRAIVAYAQYKDVGQLLPDL 2520
YDETITRRWGVDVELATPILSLQILVPSMEREQETQRLEIPSRKIFSSSSPSSSSSGST 2580
EQQFVEVFDVPKAPTSSSEQQIEDIRITAHEIPPPVSSVEQQEAASSDEDGEEREPHIRLN 2640
LDDIEFHGNSGEEVISPDSPEMLNPNYEGVSSTGSDEQPKGENEAVYRDRRLVKRQVEIT 2700
YPSEQMQQTEQVVYRSLGSPHLAQPIKLQMWLDVDSARFGPRSNPQCVRWNSFTNQWTRL 2760
GCQTEIPDFDGDFNPAAQQAILVNCSCTHISSYAVIVDVIDPEDIPEPSLLVQITSYSAF 2820
LVSLPLLLGVLLALALLRGQQTNSNTIHQNIVLCVFCAELLFFVGMQSRRQLLESEFPCK 2880
LTAICLHYFWLAAFAWTTVDYVHLYRMLTEMRDINHGPMGFYFAMGYGAPAIVVGLSVGV 2940
RAHEYGNSLFCWLSVYEPVVWWLVGPIAGMSVVNLLILFVSVKAAFTLKDHVLGFGNLRT 3000
LLWLSVVSLPLMGVMWVLAVLAASEHSQLLSLLLSGVVLLHALFCLIGYCIINKRVRENL 3060
QRTCLRCMGRKVPLLDSSMVVSNSSHNVNAAARPSNFPASGYDTTTRRNIGISASSTTSR 3120
STAKTSSSPYSDGQLRQTSTSTSNYNSASDAPSFLRGFESSTTGRSRGGEEKPSRRQRKD 3180
SDSGSETDGRSLELASSHSSDDDESRTARSSGTHRSTAVSSTPAYLPNITEHVQATTPPE 3240
LNVVQSPQLFPSVNKPVYAPRWSSQLPDAYLQSPPNIGRWSQDTGSDNEHVHGQAKMTIS 3300
PNPLPNPDLTDTSYLQQHHNKINMPPSILENIRDAREGYEDSLYGRRGEYPDKYGSYKPP 3360
SHYGSEKDYPGGGSGSQTIGHMRSFHPDAAYLSDNIYDKQRTLGSGYLGAKSESPYLSKD 3420
RITPDIYGSRDGHYSLKRQPAYATDSLHSVHSLLKNDYHQQQQQQQQQHHLQDRLSEGSDK 3480
NGYHFPYTAEEDHLPARKLSHTQPPSLHGSQLMQPPGVGLVNDVNNPGLMGRHTLNGGSR 3540
HSSRASSPPSTMVAPMQPLGPLTSITDTERNIDDDETTV
```

Fig. 5. The amino acid sequence of the Stan protein. The signal sequence is in a hatched box; nine cadherin motifs are boxed; four EGF-like motifs are shaded; two laminin G motifs are in bold; seven transmembrane domains are underlined. The nucleotide and amino acid sequence of *stan* have been deposited in GenBank under the accession number AF172329.

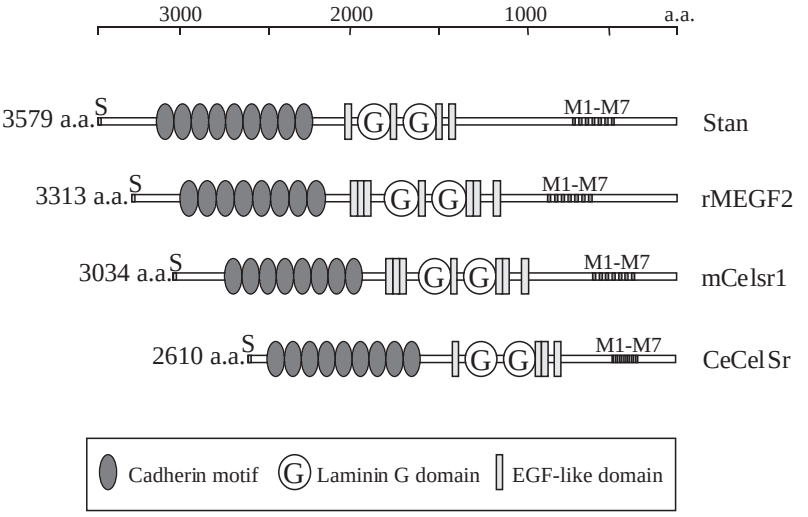

Fig. 6. Domain organization of the Stan and related proteins. MEGF2 has been identified by its multiple EGF-like domains. Northern analysis showed that it is highly expressed specifically in cerebellum and olfactory bulb (Nakayama et al., 1998). Celsr1 (Cadherin EGF LAG seven-pass G-type receptor) also appears to be implicated in the development of mammalian brain (Hadjantonakis et al., 1997). CeCelsr1 is a *C. elegans* homolog (F15B9.7). Motifs were assigned on the basis of the PROSITE analysis (Bairoch et al., 1997). The putative signal sequence and transmembrane domains are indicated by S and M, respectively.

The large size of the Stan protein provides it with many potential sites for binding to other proteins. The presence of both cadherin domains and a region whose topology is similar to a G-coupled receptor suggest that Stan could potentially function either in cell adhesion and/or in signal reception. The failure to see any evidence of altered wing cell adhesion in *stan* mutants suggests that at least in tissue polarity Stan functions primarily in signaling/signal transduction. If Stan does not function as an adhesion protein, what is the reason for the cadherin domains that are conserved in both vertebrates and invertebrates? One intriguing possibility is that the cadherin domains serve to localize the Stan protein to a plasma membrane where it functions in signal reception and/or perhaps to localize other tissue polarity proteins. Alternatively, the cadherin domains could be required for *stan* function in other tissues or for subtle but important effects on cell adhesion in the wing that we could not detect by obvious changes in clone shape.

During this work, W. J. P. was supported by a grant (G70800-GG01570) from KRF (Korea Research Foundation) and a grant (G01130) from KOSEF (Korea Science and Engineering Foundation), and P. N. A. was supported by a grant from the NIH (GM37136). S. C. and D. G. were supported by a programme grant from the British Medical research Council to M. Ashburner and D. Gubb. W.J.P conceived this work and supervised the molecular analysis of *stan*. J. C. and M. J. K. carried out most of the molecular experiments together. J. H. G took a part in the initial characterization of P1 and λ clones. S. C. and D. G. independently identified *stan* and isolated several key alleles (*stan*^{3} and *stan*^{10}), J. C. and P. N. A. independently identified *stan* and carried out most of the genetic experiments. W. J. P. and P. N. A were co-authors of the paper.

REFERENCES

Adler, P. N. (1992). The genetic control of tissue polarity in *Drosophila*. *BioEssays* **14**, 735-741.

Adler, P. N., Charlton, J. and Liu, J. (1998). Mutations in the cadherin superfamily member gene *dachsous* cause a tissue polarity phenotype by altering *frizzled* signaling. *Development* **125**, 959-968.

Adler, P. N., Charlton, J. and Park, W. J. (1994). The *Drosophila* tissue polarity gene *inturned* function prior to wing hair morphogenesis in the regulation of hair polarity and number. *Genetics* **137**, 829-836.

Adler, P. N., Krasnow, R. E. and Liu, J. (1997). Tissue polarity points from cells that have higher Frizzled levels towards cells that have lower Frizzled levels. *Curr. Biol.* **7**, 940-949.

Bairoch, A., Bucher, P. and Hofmann, K. (1997). The PROSITE database, its status in 1997. *Nucl. Acids Res.* **25**, 217-221.

Bhanot, P., Brink, M., Samos, C. H., Hsieh, J. C., Wang, Y., Macke, J. P., Andrew, D., Nathans, J. and Nusse, R. (1996). A new member of the *frizzled* family from *Drosophila* functions as a Wingless receptor. *Nature* **382**, 225-230.

Brown, N. H. and Kafatos, F. C. (1988). Functional cDNA libraries from *Drosophila* embryos. *J. Mol. Biol.* **203**, 425-437.

Clark, H. F., Brentrup, D., Schneitz, K., Bieber, A., Goodman, C. and Noll, M. (1995). *Dachsous* encodes a member of the cadherin superfamily that controls imaginal disc morphogenesis in *Drosophila***.** *Genes Dev.* **9,** 1530-1542.

Di Nocera, P. P. and Casari, G. (1987). Related polypeptides are encoded by *Drosophila* F elements, I factors, and mammalian L1 sequences. *Proc. Natl. Acad. Sci. USA* **84**, 5843-5847.

Eaton, S. (1997). Planar polarization of *Drosophila* and vertebrate epithelia. *Curr. Opin. Cell Biol.* ***9***, 860-866.

Geiger, B. and Ayalon, O. (1992). Cadherins. *Annu. Rev. Cell Biol*. **8**, 307-332.

Gho, M., Bellaiche, Y. and Schweisguth, F. (1999). Revisiting the *Drosophila* microchaete lineage: a novel intrinsically asymmetric cell division generates a glial cell. *Development* **126**, 3573-3584.

Gubb, D. (1993). Genes controlling cellular polarity in *Drosophila*. *Development* **1993 Supplement**, 269-277.

Gubb, D. and Garcia-Bellido, A. (1982). A genetic analysis of the determination of cuticular polarity during development in *Drosophila melanogaster*. *J. Embryol. Exp. Morphol.* ***68***, 37-57.

Gubb, D., Green, C., Huen, D., Coulson, D., Johnson, G., Tree, D., Collier, S. and Roote, J. (1999) The balance between isoforms of the Prickle LIM domain protein is critical for planar polarity in *Drosophila* imaginal discs. *Genes Dev.* **13**, 2315-2327.

Hadjantonakis, A. K., Formstone, C. J. and Little, P. F. R. (1998). *mCelsr1* is an evolutionarily conserved seven-pass transmembrane receptor and is expressed during mouse embryonic development. *Mech. Dev.* **78**, 91-95.

Hadjantonakis, A. K., Sheward, W. J., Harmar, A. J., de Galan, L., Hoovers, J. M. and Little, P. F. (1997). *Celsr1*, a neural-specific gene encoding an unusual seven-pass transmembrane receptor, maps to mouse chromosome 15 and human chromosome 22qter. *Genomics* **45,** 97-104.

Hartl, D. L., Nurminsky, D. I., Jones, R. W. and Lozovskaya, E. R. (1994). Genome structure and evolution in *Drosophila*: applications of the framework P1 map. *Proc. Natl. Acad. Sci. USA* **91**, 6824-6829.

Hirokawa, T., Boon-Chieng, S. and Mitagu, S. (1998). SOUSI: classification and secondary structure prediction system for membrane proteins. *Bioinformatics* **14**, 378-379.

Johnston, P. A., Archer, B. T., Robinson, K., Mignery, G. A., Jahn, R. and Sudhof, T. C. (1991). *rab3A* attachment to the synaptic vesicle membrane mediated by a conserved polyisoprenylated carboxy-terminal sequence. *Neuron* **7**, 101-109.

Klingensmith, J., Nusse, R. and Perrimon, N. (1994). The *Drosophila* segment polarity gene *dishevelled* encodes a novel protein required for response to the wingless signal. *Genes Dev.* ***8***, 118-130.

Krasnow, R. E. and Adler, P. N. (1994). A single *frizzled* protein has a dual function in tissue polarity. *Development* ***120***, 1883-1893.

Krasnow, R. E., Wong, L. L. and Adler, P. N. (1995). *dishevelled* is a component of the *frizzled* signaling pathway in *Drosophila*. *Development* ***121***, 4095-4102.

Mahoney, P. A., Weber, U., Onofrechuk, P., Biessmann, H., Bryant, P. J. and Goodman, C. S. (1991). The *fat* tumor suppressor gene in *Drosophila* encodes a novel member of the cadherin gene superfamily. *Cell* **67**, 853-868.

Nagafuchi, A. and Takeichi, M. (1988). Cell binding function of E-cadherin is regulated by the cytoplamic domain. *EMBO J.* **7**, 3679-3684.

Nakayama, M., Nakajima, D., Nagase, T., Nomura, N., Seki, N. and Ohara, O. (1998). Identification of high-molecular-weight proteins with multiple EGF-like motifs by motif-trap screening. *Genomics* **51**, 27-34.

Nielsen, H., Engelbrecht, J., Brunak, S. and von Heijne, G. (1997). A neural network method for identification of prokaryotic and eukaryotic signal peptides and prediction of their cleavage sites. *Int. J. Neural Syst.* **8**, 581-599.

Park, W. J., Liu, J., Sharp, E. J. and Adler, P. N. (1996). The *Drosophila* tissue polarity gene *inturned* acts cell autonomously and encodes a novel protein. *Development* **122**, 961-969.

Peifer, M., Rauskolb, C., Williams, M., Riggleman, B. and Wieschaus, E. (1991). The segment polarity gene *armadillo* interacts with the wingless signaling pathway in both embryonic and adult pattern formation. *Development* **111**, 1029-1043.

Reddy, G. V. and Rodrigues, V. (1999). Sibling cell fate in the *Drosophila* adult external sense organ lineage is specified by *prospero* function, which is regulated by Numb and Notch. *Development* **126**, 2083-2092.

Reifegerste, R. and Moses, K. (1999). Genetics of epithelial polarity and pattern in the *Drosophila* retina. *BioEssays* **21**, 275-285.

Rost, B., Casadio, R., Fariselli, P. and Sander, C. (1995). Prediction of helical transmembrane segments at 95% accuracy. *Protein Science* **4**, 521-533.

Sambrook, J., Fritsh, E. F. and Maniatis, T. (1989). *Molecular Cloning: A Laboratory Manual*. Cold Spring Harbor, NY: Cold Spring Harbor Laboratory Press.

Smith, R. F., Wiese, B. A., Wojzynski, M. K., Davison, D. B. and Worley, K. C. (1996). BCM search launcher – an integrated interface to molecular biology data base search and analysis services available on the world wide web. *Genome Res*. **6**, 454-462.

Tautz, D. and Pfeiffle, C. (1989). A nonradioactive in situ hybridization method for the localization of specific RNAs in *Drosophila* embryos reveals a translational control of the segmentation gene *hunchback*. *Chromosoma* **98**, 81-85.

Taylor, J., Abramova, N., Charlton, J. and Adler, P. N. (1998). *Van Gogh*: a new *Drosophila* tissue polarity gene. *Genetics* **150**, 199-210.

Tepass, U., Gruszynski-Defeo, E., Haag, T. A., Omatyar, L., Torok, T. and Hartenstein, V. (1996). *shotgun* encodes *Drosophila* E-Cadherin and is preferentially required during cell rearrangement in the neurectoderm and other morphogenetically active epithelia. *Genes Dev*. **10**, 672-685.

Theisen, H., Purcell, J., Bennett, M., Kansagara, D., Sved, A. and Marsh, J. L. (1994). *dishevelled* is required during wingless signaling to establish both cell polarity and cell identity. *Development* **120**, 347-360.

Uemura, T., Oda, H., Kraut, R., Hayashi, S., Kotaoka, Y. and Takeichi, M. (1996). Zygotic *Drosophila* E-cadherin expression is required for processes of dynamic epithelial cell rearrangement in the *Drosophila* embryo. *Genes Dev.* **10**, 659-671.

Usui, T., Shima, Y., Shimada, Y., Hirono, S., Burgess, R. W., Schwarz, T. L., Takeichi, M. and Uemura, T. (1999). Flamingo, a seven-pass transmembrane cadherin, regulates planar cell polarity under the control of Frizzled. *Cell* **98**, 585-595.

Wherli, M. and Tomlinson, A. (1998). Independent regulation of anterior/posterior and equatorial/polar polarity in the *Drosophila* eye. *Development* **125**, 1421-1432.

Wolff, T. and Rubin, G. M. (1998). s*trabismus*, a novel gene that regulates tissue polarity and cell fate decisions in *Drosophila*. *Development* **125**, 1149-1159.

Wong, L. L., and Adler, P. N. (1993). Tissue polarity genes of *Drosophila* regulate the subcellular location for prehair initiation in pupal wing cells. *J. Cell Biol.* **123**, 209-221.

Xu, T. and Rubin, G. M. (1993). Analysis of genetic mosaics in developing and adult *Drosophila* tissues. *Development* **117**, 1223-1237.